ACCOUNTS of chemical research

Article

pubs.acs.org/accounts

Synthesis and Defect Investigation of Two-Dimensional Molybdenum Disulfide Atomic Layers

Published as part of the Accounts of Chemical Research special issue "2D Nanomaterials beyond Graphene".

Sina Najmaei, Jiangtan Yuan, Jing Zhang, Pulickel Ajayan, and Jun Lou*

Department of Materials Science and NanoEngineering, Rice University, Houston, Texas 77005, United States

CONSPECTUS: The unique physical properties of two-dimensional (2D) molybdenum disulfide (MoS_2) and its promising applications in future optoelectronics have motivated an extensive study of its physical properties. However, a major limiting factor in investigation of 2D MoS_2 is its large area and high quality preparation. The existence of various types of defects in MoS_2 also makes the characterization of defect types and the understanding of their roles in the physical properties of this material of critical importance.

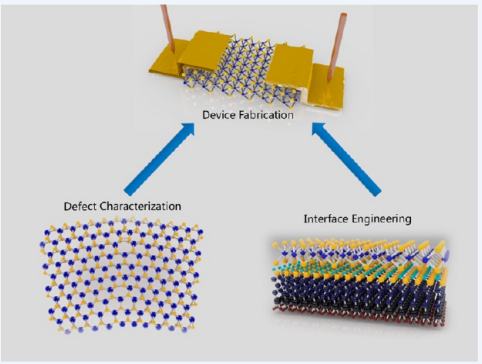

In this Account, we review the progress in the development of synthetic approaches for preparation of 2D MoS_2 and the understanding of the role of defects in its electronic and optical properties. We first examine our research efforts in understanding exfoliation, direct sulfurization, and chemical vapor deposition (CVD) of MoS_2 monolayers as main approaches for preparation of such atomic layers. Recognizing that a natural consequence of the synthetic approaches is the addition of sources of defects, we initially focus on identifying these imperfections with intrinsic and extrinsic origins in CVD MoS_2. We reveal the predominant types of point and grain boundary defects in the crystal structure of polycrystalline MoS_2 using transmission electron microscopy (TEM) and understand how they modify the electronic band structure of this material using first-principles-calculations. Our observations and calculations reveal the main types of vacancy defects, substitutional defects, and dislocation cores at the grain boundaries (GBs) of MoS_2. Since the sources of defects in two-dimensional atomic layers can, in principle, be controlled and studied with more precision compared with their bulk counterparts, understanding their roles in the physical properties of this material may provide opportunities for changing their properties. Therefore, we next examine the general electronic properties of single-crystalline 2D MoS_2 and study the role of GBs in the electrical transport and photoluminescence properties of its polycrystalline counterparts. These results reveal the important role played by point defects and GBs in affecting charge carrier mobility and excitonic properties of these atomic layers.

In addition to the intrinsic defects, growth process induced substrate impurities and strain induced band structure perturbations are revealed as major sources of disorder in CVD grown 2D MoS_2. We further explore substrate defects for modification and control of electronic and optical properties of 2D MoS_2 through interface engineering. Self-assembled monolayer based interface modification, as a versatile technique adaptable to different conventional and flexible substrates, is used to promote significant tunability in the key MoS_2 field-effect device parameters. This approach provides a powerful tool for modification of native substrate defect characteristics and allows for a wide range of property modulations. Our results signify the role of intrinsic and extrinsic defects in the physical properties of MoS_2 and unveil strategies that can utilize these characteristics.

INTRODUCTION

The field-effect electronic properties, thickness-dependent band structure, light emitting properties, and spin coupling properties of molybdenum disulfide (MoS_2) have motivated an immense effort in understanding its physical and chemical properties.[1−8] Additionally, MoS_2 atomic layers show remarkable tunability in their physical properties that holds great promise in future electronics and optics.[4,9−11] However, a bottleneck in fully exploring MoS_2 properties and applications has been its large-area and high-quality synthesis. This has made the study of synthetic processes and defect characterization of this material the center point in this research area.[12−15]

Introduction of new scattering sources, such as interface defects and surface optical phonons, is unique in 2D materials, modifying their electronic and optical characteristics.[16−19] Since these properties as well as the intrinsic structural defects in 2D materials are in principle more controllable, they can be systematically exploited to design strategies for material property modifications.[20,21]

In this Account, we will discuss the synthetic approaches for 2D MoS_2 preparation and examine the defect characteristics of the products. By understanding the role of defects in physical properties of MoS_2, we reveal their importance. We further utilize our acquired knowledge to propose and implement

Special Issue: 2D Nanomaterials beyond Graphene

Received: August 7, 2014
Published: December 9, 2014

DOI: 10.1021/ar500291j
Acc. Chem. Res. 2015, 48, 31−40

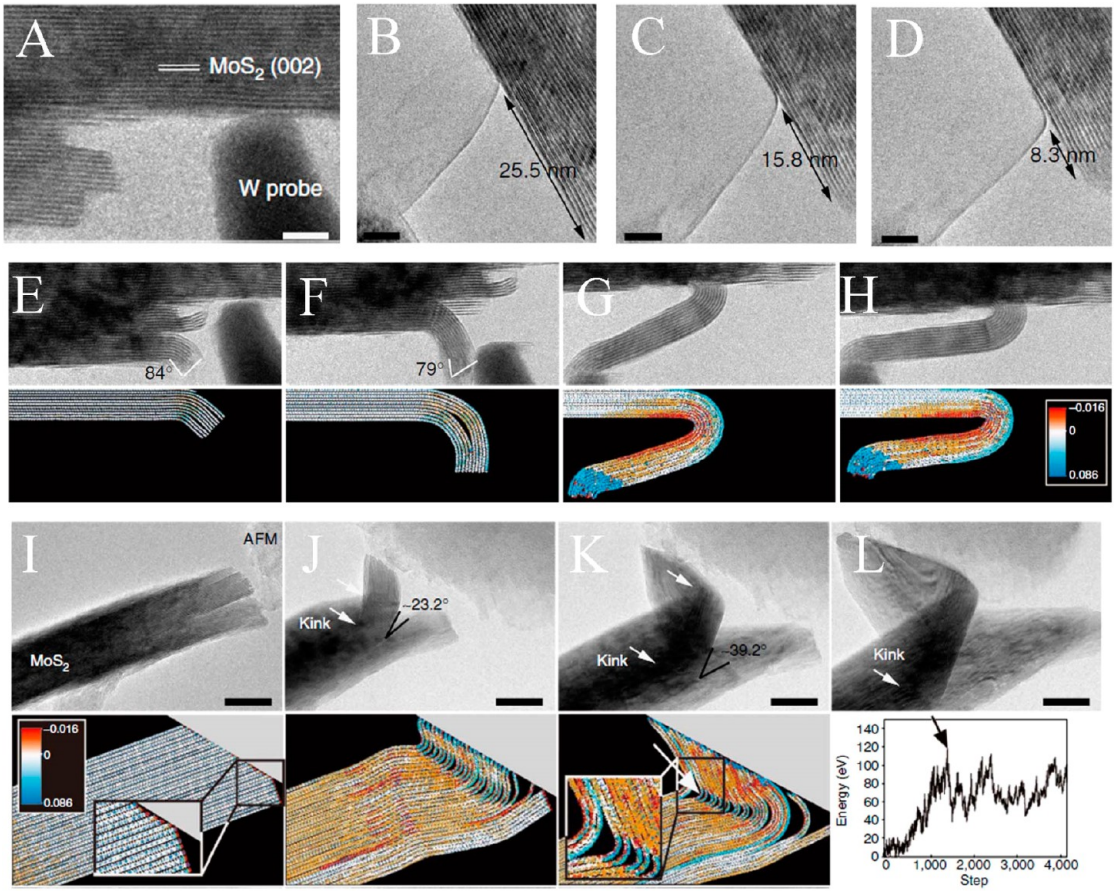

Figure 1. Mechanical exfoliation and bending processes in MoS_2 atomic layers. (A) Experimental setup showing a tungsten tip brought in contact with bulk MoS_2 crystal. (B–D) The cleavage process of a monolayer MoS_2. (E–H) The cleavage process in 11 layered samples with the MD simulations. The homogeneous curving and rippling in thinner samples (<5 layers) is converted to interlayer sliding. (I–L) For thicker samples (>20 layers) kinking and intense plasticity is apparent in both experiments and MD simulations. Adapted with permission from ref 26. Copyright 2014 Nature Publishing Group.

defect engineering strategies to control material properties in two-dimensional systems.

TWO-DIMENSIONAL MoS_2 SYNTHESIS AND PREPARATION

The family of van der Waals solids including MoS_2 is structurally distinct because of their weak interlayer interactions. This results in anisotropies in their optical, electrical, and mechanical properties that are accompanied by major thickness dependency in the quantum confinement regime.[1,2,5−7,11,22,23] However, exploitation of these properties is made possible through the isolation of their chemically and mechanically stable monolayers.[24−26] Exfoliation was early on the only method for small-scale production of 2D materials.[24,25] To understand the exfoliation process we recently examined the interlayer interactions in MoS_2 using in situ TEM experiments measuring and demonstrating the distinctive characteristics of the exfoliation process in MoS_2 atomic layers (Figure 1).[26]

We used a tungsten probe to selectively contact, cleave, and bend MoS_2 atomic layers (Figure 1A). We demonstrate that the exfoliation and mechanical properties of MoS_2 atomic layers are highly thickness-dependent. Few layered samples tend to be very flexible with very little damage to the samples over large bending regimes (Figures 1B–D). However, as the thickness of the materials is increased (>5 layers) the homogeneous bending and rippling is transformed into interlayer sliding (Figure 1E–H) and to kinking beyond these thicknesses (>20 layers) (Figure 1I–L). These results demonstrate the advantages of mono- and few-layer samples in flexible electronic applications and also the challenges in exfoliation of MoS_2. Despite the ease of exfoliation for high quality sample preparation, it entails lack of control and somewhat unreliable nature for large-scale material production. However, the knowledge acquired from these experiments can help to establish more systematic approaches based on the exfoliation process. This also exemplifies the need for development of bottom-up synthetic approaches for further exploration of these materials. In the next section, two major chemical synthesis approaches for preparation of MoS_2 will be described.

Synthesis of large area MoS_2 is possible through a simple solid phase sulfurization (SPS) of molybdenum thin films (Figure 2A,B).[13] However, the kinetics of growth and limitations in deposition of thin continuous layers of molybdenum are major challenges. Dark-field TEM images and diffraction patterns acquired from these samples show a high level of polycrystalinity with grain sizes in the range of 10 to 30 nm (Figure 2C–F).

The existence of large density of point and grain boundary defects in the SPS MoS_2 samples results in their poor electrical performance. This results in typically poor room temperature field-effect mobilities (0.004–0.04 $cm^2\ V^{-1}\ s^{-1}$) compared with mechanically exfoliated samples (0.1–10 $cm^2\ V^{-1}\ s^{-1}$).[13] A

DOI: 10.1021/ar500291j
Acc. Chem. Res. 2015, 48, 31−40

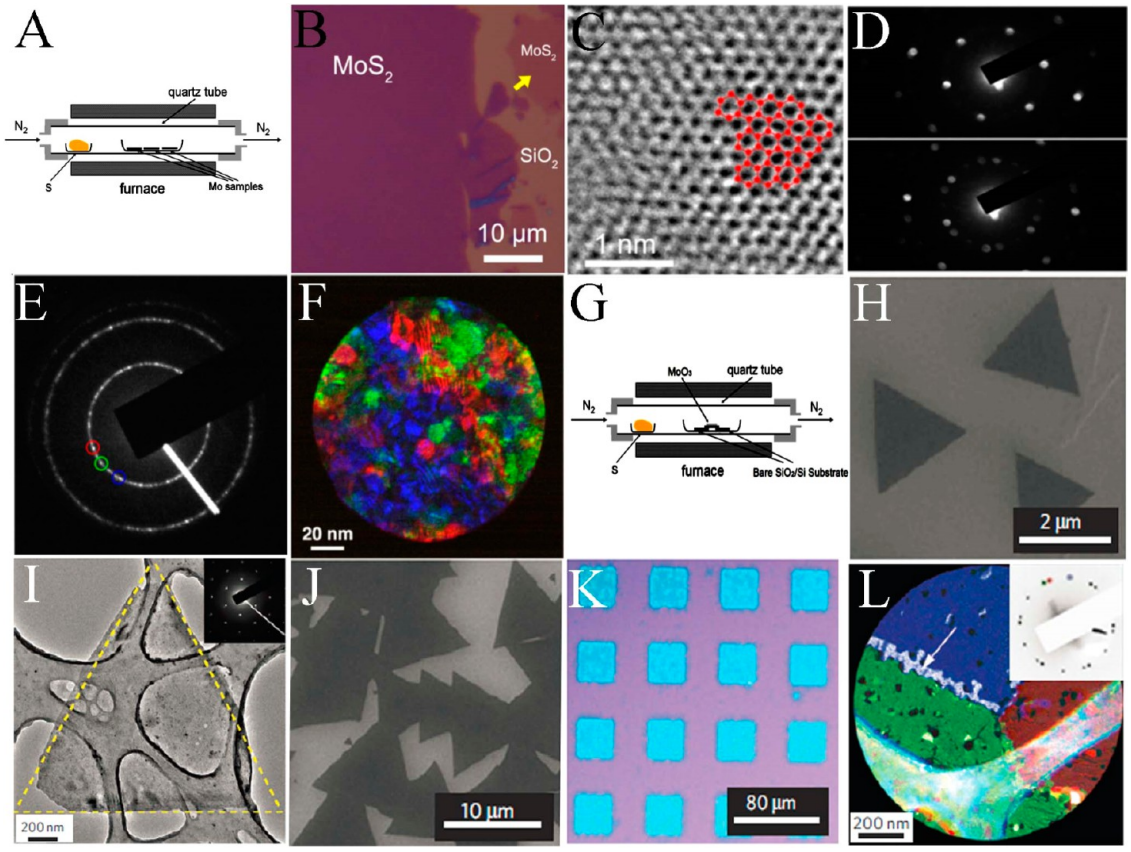

Figure 2. Two distinctive chemical approaches to grow 2D MoS_2. (A) The configuration of substrates and precursors in the SPS approach. Here e-beam evaporated molybdenum films are positioned in the center of the furnace and exposed to sulfur at elevated temperature. (B) Large area films grown using SPS. (C) High resolution TEM image of the material. (D) Diffraction patterns acquired from small regions at different locations showing the 6-fold symmetry related to MoS_2 atomic structure. (E) The diffraction pattern acquired from a large area of the material showing many different crystalline orientations. (F) The color coded dark-field TEM image shows the grain orientation distribution and the grain sizes (~10−20 nm). (G) CVD growth configuration. (H) Nucleation of small single-crystalline domains of monolayer MoS_2 in low precursor regime of growth. (I) The TEM image and the diffraction pattern acquired from one triangular domain proving its single crystallinity. (J) In higher nucleation and precursor supply conditions, the triangular domains grow and merge resulting in semicontinuous films. (K) Patterned substrates for promotion of nucleation can significantly enhance the growth. (L) The dark-field images acquired from the CVD-grown sample color coded here show grain sizes in the tens of micrometer range. Adapted with permission from ref 12 (Copyright 2013 Nature Publishing Group) and ref 13 (Copyright 2012 WILEY-VCH Verlag GmbH & Co. KGaA, Weinheim).

combination of DC and AC conductivity analysis on these MoS_2 samples reveals significant localizations that result in electron hopping near the Fermi level through the quantum mechanical tunneling modes.[13,27] Despite the degrading effects of defects on the transport properties of MoS_2, they may be useful in other applications such as electrochemical catalysis.[28] Alternatively, a solution to the limitations associated with the direct sulfurization method is a complete vapor-phase strategy.

Taking advantage of low melting and evaporation temperatures of MoO_3 as a precursor, vapor phase sulfurization of MoS_2 is achievable.[12] With the precursor supply control, the general nucleation and growth mechanisms in MoS_2 can be revealed (Figure 2G−K). The experiments showed that the MoS_2 synthesis was limited by the diffusion of vapor-phase MoO_{3-x}: decreasing the density of dispersed MoO_3 nanoribbons systematically slowed or stopped the growth at certain points. Initially, small single-crystalline triangular domains nucleate on the bare substrate (Figure 2H,I), followed by the formation of a partially continuous film with grain boundary formation when two or more domains meet (Figure 2J). This process would eventually extend into large-area single-layered continuous MoS_2 films if sufficient precursor supply and denser nucleation sites were provided. In the growth process, it is found that MoS_2 triangular domains and films are commonly nucleated and formed in the vicinity of the substrates' edges, scratches, dust particles, or rough surfaces. Based on this discovery, MoS_2 nucleation sites can thus be controlled by creating step edges on substrates using conventional lithography processes (Figure 2K). This simple strategy provides a robust route for the growth of centimeter sized, high-quality MoS_2 monolayers with grain sizes in the range of 15−30 μm (Figure 2L), which can be readily transferred to any substrates or directly used to fabricate devices. Our postgrowth measurements on film thicknesses range from single to multiple layers, while mobility measurements obtained show an average of 4.3 ± 0.8 $cm^2\ V^{-1}\ s^{-1}$ for multiple devices. This result shows great improvement from solid-phase sulfurized samples and is comparable to that of mechanically exfoliated samples.[25] However, the wide range of the measured field-effect mobilities and the differences between these measurements and that of bulk materials deserve more attention.[29] We next inspect the intrinsic and extrinsic sources for mobility degradation in CVD-MoS_2.

DOI: 10.1021/ar500291j
Acc. Chem. Res. 2015, 48, 31−40

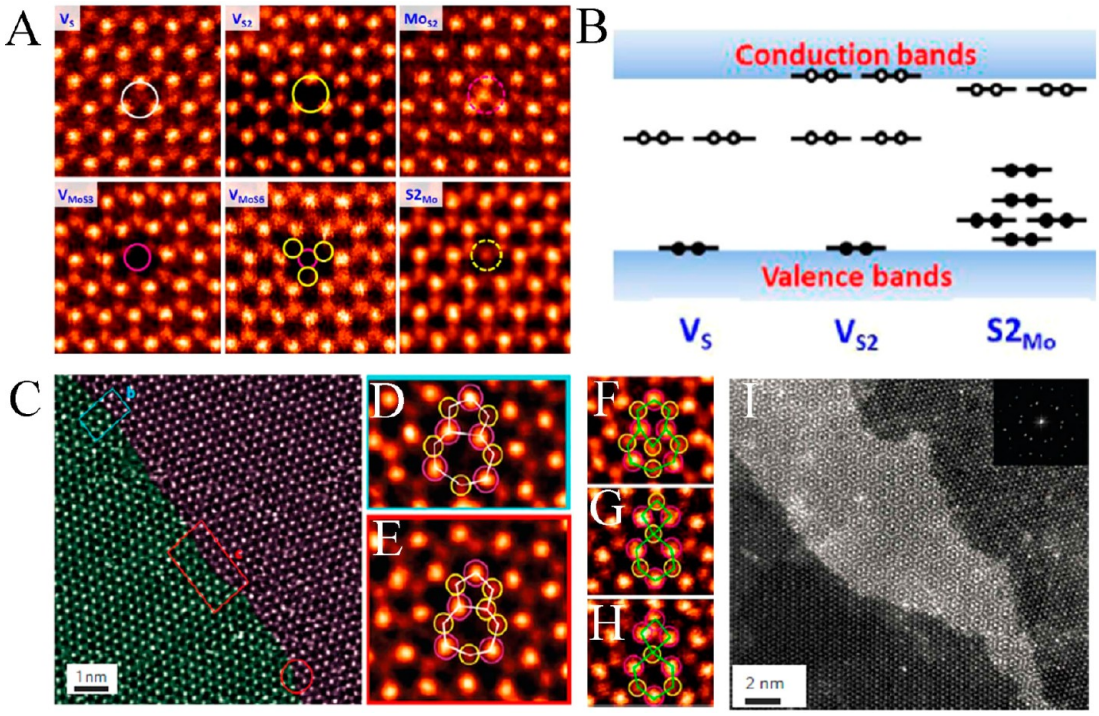

Figure 3. Point, substitutional, and grain boundary defects in MoS_2. (A) Several types of point and substitution defects shown here in these TEM images are commonly seen in CVD 2D MoS_2. (B) The most prominent types of defects resulting in acceptor deep states below the conduction band of MoS_2. (C) A TEM image of a conventional grain boundary consisting of dislocation cores patching the two grains. (D) The TEM images of the most common 5|7 ring dislocation core observed in MoS_2 and (E) one of its center Mo atoms substituted with two sulfur atoms. (F−H) The TEM images of other commonly observed dislocation cores in MoS_2. (I) The TEM image acquired from regions with over layer growth without any chemical stitching. Adapted with permission from ref 12 (Copyright 2013 Nature Publishing Group) and ref 30 (Copyright 2013 American Chemical Society).

INTRINSIC DEFECTS IN TWO-DIMENSIONAL MoS_2

Defects are inevitable to the growth of materials due to imperfections of the synthetic process, and this certainly applies to the growth of MoS_2 atomic layers.[12,30] The molecular configuration of MoS_2 allows for six commonly observed types of point defects. These include monosulfur vacancies (V_S), disulfur vacancies (V_{S2}), vacancy complexes of Mo and three nearby sulfurs (V_{MoS3}) and Mo and the nearby three disulfur pairs (V_{MoS6}), and antisite defects where a Mo atom substitutes the S_2 column (Mo_{S2}) or a S_2 column substitutes a Mo atom ($S2_{Mo}$) (Figure 3A). Based on density functional theory (DFT) calculations, in the whole range of S chemical potential, V_S is found to have the lowest formation energy, while Mo_{S2} and $S2_{Mo}$ antisite defects are among the highest formation energies under S-rich and Mo-rich environments, respectively.[30] This calculation is consistent with the experimental observations, where V_S is frequently observed in all samples, but antisite defects were only occasionally found. Simulations also show that point-defects influence the electronic properties of MoS_2. Both V_S and V_{S2} introduce unoccupied deep levels about 0.6 eV below the conduction band minimum (CBM) (Figure 3B). These states act as compensation centers in n-type MoS_2 and can trap charges and transform into scattering centers.

When grains meet, their coalescence leads to formation of GBs composed of dislocation arrays of pristine and sulfur-substituted 5|7-fold rings (Figure 3C−E).[12,30,31] The rings comprise Mo-oriented dislocation core structures formed by 15 atoms, with two Mo atoms constituting a Mo−Mo bond shared by the 5- and 7-fold rings. There are five distinct Mo sites that could be substituted by S atoms in each dislocation. However, besides the conventional 5|7-fold rings, other core structures such as 4|4-, 4|6-, 4|8-, and 6|8-fold rings can also be observed (Figures 3 F−H). Taking 5|7 structure as the basic dislocation core structure, one can generate the 6|8 structures by the addition of monosulfurs or disulfurs into the Mo−Mo bonds, and 4|6 structures can be derived from S-oriented 5|7 structures by removing two S atoms, which are energetically favorable under S-rich and Mo-rich conditions, respectively. This diverse set of dislocation cores can show varied properties. The ideal 4|4 GBs show perfect metallicity; however, kinks can induce significant disturbance to the electronic behavior of the grain boundaries. In the extreme case of 4|8 grain boundaries, localized midgap states right above the top of the MoS_2 valence band will be introduced. As well as the aforementioned traditional grain boundaries, overlapped junctions may also form when two MoS_2 grains merge (Figure 3I). Two grains will continue to grow on top of each other to form a bilayered overlapped region at the junction, where the distinct moiré pattern can be observed. The structural richness of point defects and GBs in MoS_2 suggest exciting possibilities of controlling the defect characteristics and the local properties in MoS_2. This motivates our studies to better understand the direct influence of defects such as GBs on MoS_2 electron transport properties.

ELECTRICAL PERFORMANCE OF CVD SINGLE-CRYSTALLINE AND POLYCRYSTALLINE MoS_2

On the basis of field-effect channel-length dependent transport studies on single-crystalline monolayers of MoS_2, we unveil

DOI: 10.1021/ar500291j
Acc. Chem. Res. 2015, 48, 31−40

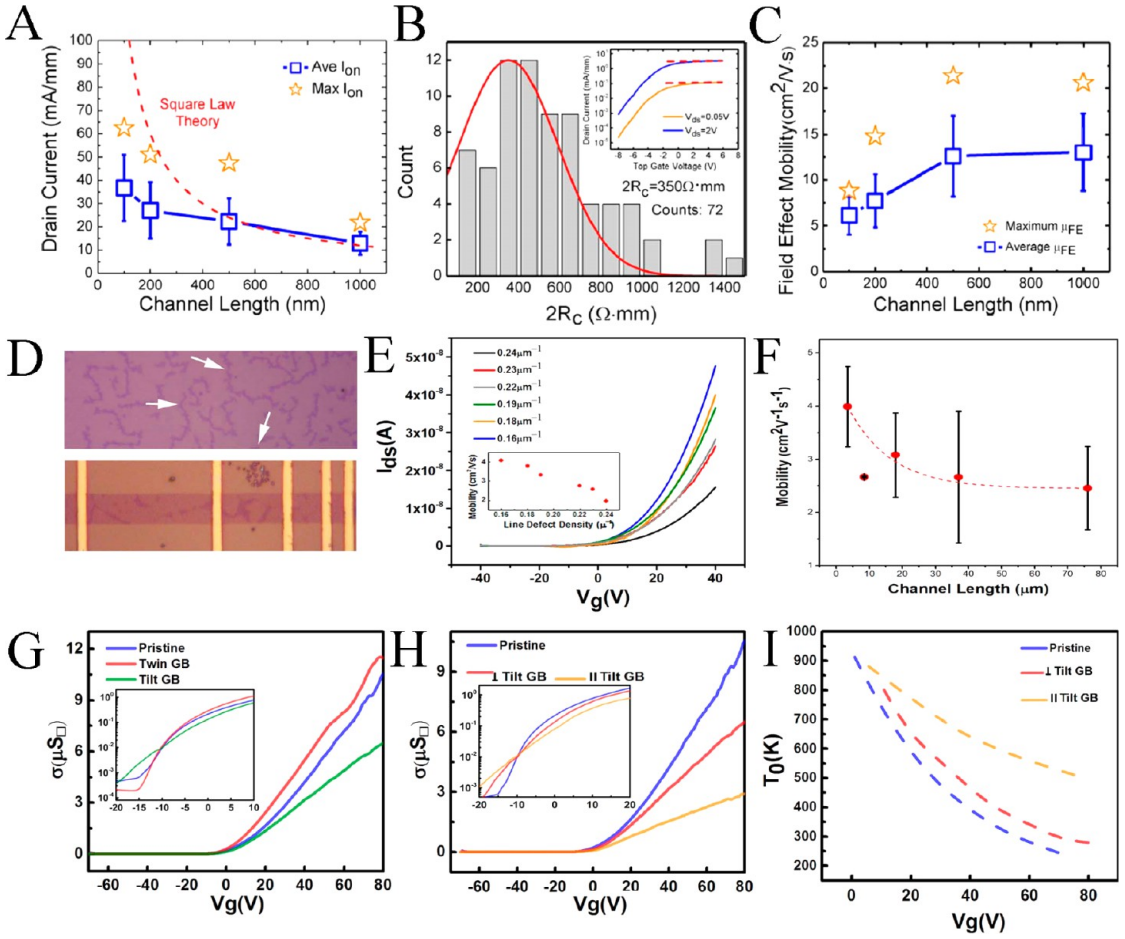

Figure 4. Role of defects in MoS_2 electron transport. (A–C) The changes in current density, contact resistance, and field-effect mobilities in the CVD single-crystalline MoS_2 as a function of channel length. (D) The optical micrograph of MoS_2 large-area films and device design. The bilayered regions, indicated by white arrows are associated with the GBs. The collective role of GBs in the transport properties of MoS_2 extracted from measurements on devices with (E) similar and (F) varied channel lengths. (G) The electrical transport measurements on individual GBs focusing on merged triangular domains with tilt and twin-180 GBs (H) Transport properties of the devices made parallel or vertical to the tilt GBs. (I) Low temperature measurements and comparison of variable range hopping coefficients for different orientations measurements described in panel H. Adapted with permission from ref 34 (Copyrights 2014 American Chemical Society) and ref 32 (Copyright 2013 American Chemical Society).

important characteristics of CVD samples.[32] Despite high current densities at large channel lengths, device contact resistance is a major challenge (~175 Ω·cm per contact) (Figure 4A,B). It dominates the device performances at low channel lengths (<500 nm) ,and device performance deviates from the predicted values (Figure 4A,B). The charge carrier mobilities of the samples improve when encapsulated in alumina because the high dielectric environment suppresses the substrate impurity scattering ($\mu \approx 10$ cm^2/(V s); Figure 4C). By elimination of the contact resistance, the mobilities can be further improved (~22 cm^2/(V s)). The temperature dependent measurements on MoS_2 samples resolve strong localization that can be partially relieved by high dielectric encapsulation.[33] However, these measurements exclude an important source of scattering, that is, grain boundaries (GBs) in polycrystalline CVD-MoS_2. Next we will consider the role of GBs in MoS_2 electron transport.

We explore the collective and individual role of GBs on the electrical properties of MoS_2.[34] We first need to develop techniques that allow us to identify, quantify, and vary the density of GBs in the device channel material. Variations in optical response of the material, despite the lack of knowledge about their origins, have previously been used for identification of GBs.[35] However, in large-area monolayer MoS_2, the bilayer regions formed by preferred second layer growth along GBs can also be used for this purpose (Figure 4D). We use these bilayered markers, visible in optical and Raman maps, as an approximate measure for quantification of nominal line-defect densities in large-area films. We made several devices with similar channel lengths and quantified the line-defect densities by measuring the total length of the bilayered regions and dividing it by the channel area. These experiments show a decrease by half in the magnitude of mobilities as the nominal line-defect densities increase from 0.16 to 0.24 μ^{-1} (Figure 4E). To systematically control the line-defect densities, we examine the channel-length dependency of the transport properties. Having in mind that shorter channels have a lower chance of containing a grain boundary, we demonstrate a statistical increase in the line-defect densities of the devices as the channel length increases. These experiments show a consistent decrease in charge carrier field-effect mobilities as the channel length and the corresponding line-defect densities increase (Figure 4F).

To complement these collective studies, we also identify and quantify the role of individual GBs using devices made on merged single-crystalline triangular domains. Through the TEM analysis of GBs, one can divide them into two major

DOI: 10.1021/ar500291j
Acc. Chem. Res. 2015, 48, 31–40

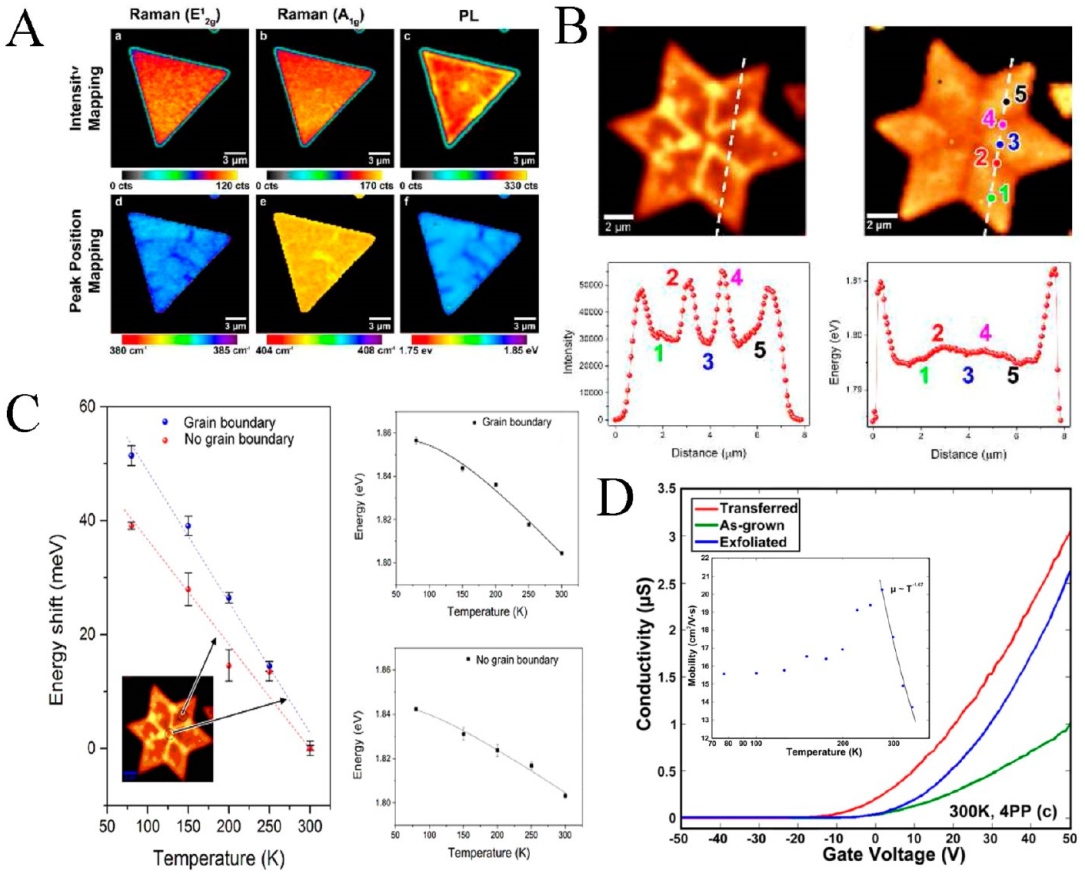

Figure 5. Growth related extrinsic sources of defects. (A) Raman and PL maps from single crystals of MoS_2. (B) PL intensity and peak position maps of polycrystalline MoS_2 and the line profile from these maps. (C) Temperature-dependence of PL position in regions with and without GBs. (D) Transfer curves acquired from as-grown and transferred CVD samples and the temperature dependency of field-effect mobility in as-grown samples (inset). Adapted with permission from ref 42 (Copyright 2014 Nature Publishing Group) and ref 33 Copyrights 2013 AIP Publishing LLC.

types, tilt and 180-twin boundaries. We made several devices on these types of GBs, as well as pristine single crystals, of 2D MoS_2 and measured the transfer characteristics of the devices. This unveils a general behavior for transport across the grain boundary. Tilt GBs tend to degrade the electronic transport properties, while 180-twin boundaries are not affected (Figure 4G). The magnitude of field-effect mobility changes in devices made on the tilt GBs is reduced by roughly half compared with pristine single crystals. Electronic transport across and parallel to these GBs reveals an interesting anomaly (Figure 4H). The electron transport parallel to the tilt GBs is more affected than the transport across them. To explain this, we suggest that the source of scattering is not the dislocation cores at the GBs, and we hypothesize that instead it is a result of higher accumulation densities of defects close to the GBs. This way the devices made parallel to the boundary regions contain a larger density of defects in the electron pathway and will degrade the transport behavior more significantly. We test this hypothesis by examining the low-temperature transport behaviors in these devices. By fitting the different temperature regimes of transport into variable-range- and nearest-neighbor-hopping mechanisms, we extract two important constants (Figure 4I). The comparison of the high temperature regime constants acquired from measurements in different configurations of tilt GBs and pristine single-crystals reveals that indeed the density of sources of scattering increases close to the tilt GBs. Our analysis indicates a good agreement between the parameters in our model and theoretically estimated point-defect localization lengths in MoS_2, confirming them as the source of scattering close to the tilt boundaries (Figure 4I). Additional Raman spectroscopy experiments from GB regions identify their chemical instability and further confirm our point-defect accumulation hypothesis.[31]

GROWTH INDUCED EXTRINSIC DEFECTS

In addition to the MoS_2 intrinsic structural defects, the surface impurities and interface dangling bonds are known to have a substantial role in the transport properties of these atomic layers.[18,19,36] The modification of electrical properties of 2D MoS_2 as a result of GBs was accompanied by changes in photoluminescence (PL) of the material. However, the variation in MoS_2 PL response is not specific to the location of GBs and systematic changes have been observed in its single crystals.[37] In Figure 5A, one can see that even in monolayer MoS_2 single crystals clear contrast line features vertical to the triangle sides appear in the PL peak position and intensity maps. This is clearly not a result of GBs and we attribute the changes to the strain accumulated in the material during the growth because there is a difference between the thermal properties of MoS_2 and silicon/silica substrates. We estimate the changes in the MoS_2 bandgap as a result of tensile strain using first-principles calculations, and from this, we can evaluate the strain levels in the material. These experiments show that the inhomogeneous strain fields in the order of 0.2% relative to the rest of the material are present in the as-grown samples. This was further confirmed because the local variations

DOI: 10.1021/ar500291j
Acc. Chem. Res. 2015, 48, 31−40

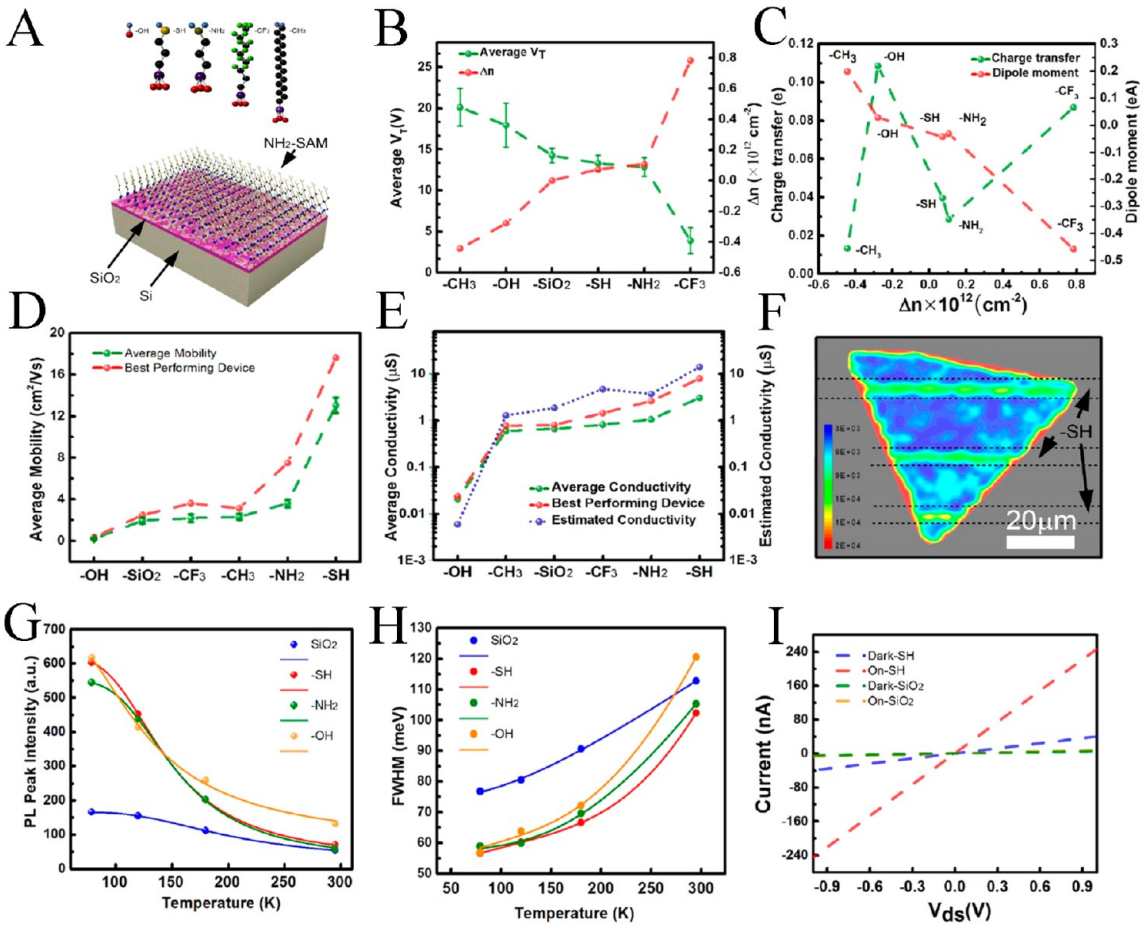

Figure 6. Interface engineering and its role on physical properties of 2D MoS_2. (A) Schematic illustration of the molecular chains and their assembly on the Si/SiO_2 substrates. (B) The average threshold voltage for devices on varied substrates in green and their corresponding doping level changes in red. (C) The charge transfer changes calculated using DFT calculation and molecular dipole moment in each molecule. (D) The average field-effect mobility in devices made on varied substrates. (E) The average conductivity of devices at gate voltage of 40 V. (F) The PL intensity map acquired from a MoS_2 triangular domain transferred to a patterned substrate. The pattern regions are functionalized with thiol terminated SAMs. (G) The temperature-dependency of PL intensity indicating the major role of substrates. (H) The PL line width on different substrates. (I) The photocurrent acquired under dark and illumination conditions. Adapted with permission from ref 21. Copyrights 2014 American Chemical Society.

vanished after transfer of the monolayers to a new substrate. The inhomogeneities in the PL response of the material are accompanied by a universal shift, which we attributed to 1% global strain in the material. These studies determine the role of high temperature growth in modifying properties of pristine single-crystalline materials.

Examination of PL characteristics of polycrystalline samples has shown enhanced contrast at the GBs (Figure 5B). The extended regions of the modified PL responses at the GBs, spanning fractions of a micrometer indicate that reasons beyond dislocation cores at the GBs are responsible for the observed effects, similar to conclusions reached for the role of GBs in the electrical properties of MoS_2. Many arguments have been put forward about the underlying mechanism for this type of PL modulations at the GBs; however a clear and complete picture still remains elusive. We demonstrate the importance of strain as an additional factor contributing to the observed PL behaviors at the GBs. Our temperature-dependent PL study of GBs and single-crystalline regions of MoS_2 show that both follow Varshni's law for bandgap temperature dependency (Figure 5C). This is a clear indication that localizations as a result of point-defects cannot solely explain the effects observed. However, the parameters of this fitting indicate a softening of the phonon modes that can be a result of the suggested strain at the GBs.

In addition to growth induced strain, other growth related artifacts affecting MoS_2 properties can also have extrinsic origins. Surface contamination and substrate property modification are major contributors to the changes in the physical properties of as-grown samples. In fact our experiments on the as-grown samples compared with transferred samples indicate a substantial increase in substrate defects as a result of high temperature growth on the as-grown substrates (Figure 5D). Transfer of samples to new substrates can improve the properties of the single crystals and make them comparable to exfoliated samples. Low temperature measurements also reveal the single-crystal MoS_2 mobility profile. These results show enhanced impurity scattering and localizations in case of as-grown samples, which vindicate the effects of growth related extrinsic impurity characteristics on electron transport.

■ INTERFACE ENGINEERING

Substrate plays a major role in the physical properties of 2D materials and can modify the intrinsic properties of MoS_2. As a result, interface engineering strategies, by modifying and controlling the substrate chemistry, may be a simple and

DOI: 10.1021/ar500291j
Acc. Chem. Res. 2015, 48, 31−40

robust approach to tune MoS_2 properties. Study of interfaces is a classical area of research in bulk materials.[38,39] The challenges with interfaces are more significant in 2D materials because the surface dominates their properties. As a consequence, in the monolayer regime, relatively lower mobilities of charge carrier compared with their bulk counterparts are expected. These effects in MoS_2 have been attributed to trap states originating from vacancy and interface defect states.[18,19] Consequently, understanding the localized band tails at the bottom of conduction band or top of valence band becomes important in interpreting the nature of electronic transport in this material.[40] This has resulted in several studies of interface engineering in order to control and manipulate the shape and extent of band tails in the forbidden gap of MoS_2 by healing or modifying the trap states.[21,41]

To explore interface engineering in MoS_2 atomic layers, a versatile approach adaptable to conventional oxides and flexible platforms that systematically controls important device parameters will be discussed. A substrate passivation scheme based on self-assembly of molecular monolayers with a diverse chemistry is utilized and studied to demonstrate such properties.[21] The assembled molecules have a diverse range of chemical and physical properties resulting in significant control over the modulations of the electron transport and optical properties of 2D MoS_2.

It is known that the point defects in the SiO_2 substrate result in deep states in the forbidden gap of MoS_2. These deep states can trap charges and create localization in the material resulting in different regimes of transport and scattering mechanisms at different temperatures. Interface defect passivation results in trapping and scattering character modification, and understanding the role they play is vital in precise control of 2D MoS_2 properties. To explore the role of substrate chemistry in the electronic transport properties of MoS_2, we passivate SiO_2 substrates with a variety of organosilane self-assembled monolayers (SAM) with different end groups (thiol (−SH), amine ($-NH_2$), methyl (CH_3), and fluoro (CF_2)) (Figure 6A). These results were compared with pristine and −OH terminated SiO_2 substrates. The tunability in threshold voltage of gate tuned transfer curves indicates variations in doping levels of the samples. We estimate the doping levels using the threshold voltage and a capacitor model arriving at a quantitative representation of the substrate doping effects (Figure 6B). The charge transfer alone, estimated between MoS_2 and its substrate using DFT calculations, does not explain the measured values and in all molecules a charge accumulation at the interface should be anticipated. However, the dipole characteristics of the molecules contribute more selectively as they have very different magnitudes and directions thus making significant contribution to MoS_2 doping and charge trapping (Figure 6C).

The field-effect mobilities estimated for these devices show remarkable tunability as a function of SAM end groups (Figure 6D). The best performing devices from the perspective of field-effect mobility are the devices made on thiol-terminated SAMs, an increase of roughly 4 times in mobility compared with samples on SiO_2 substrates. The conductivities show a consistent trend following the free electron model (Figure 6E). The effects of these substrate modifications are also significant in the PL properties. We use the photolithography technique to pattern the SAMs on the substrate. The differences between the modified and pristine regions of the substrate can be clearly distinguished in the PL maps (Figure 6F). The PL signals from the SAM modified regions of the substrate are significantly enhanced compared with pristine areas. The PL characteristics of monolayer MoS_2 on different SAMs, examined using temperature-dependent measurements, shows that these samples follow Varshni's law for bandgap temperature dependency. Therefore, no band structure modification in the material is expected as a function of changes in the structural-defect characteristics and localizations as the substrates are changed. However, the PL peak intensity and fwhm show significant differences reflecting on the role of defect characteristics of the substrates (Figure 6G,H). Passivated substrates tend to have a lower defect mediated nonradiative decay that results in higher and narrower PL emission lines. The combinations of these electrical and optical modifications on the passivated substrates result in enhanced photocurrent in the devices (Figure 6I).

■ CONCLUSIONS

In this Account, we demonstrate our successes with understanding of the growth and preparation of MoS_2 atomic layers. We examine the structural characteristics and the degrading effects of intrinsic and extrinsic defects in the electronic and optical properties of CVD MoS_2. We demonstrate that beyond the intrinsic defects the interface impurities play a very important role in the MoS_2 properties.

There are ample challenges remaining in understanding the growth process and defect formation in 2D MoS_2 and other transition metal dichalcogenides. Studying and promoting the nucleation and growth, surface absorption, and defect detection techniques can establish a strong foundation to identify effective strategies for modification and utilization of defects properties in physical property control of 2D materials.

■ AUTHOR INFORMATION

Corresponding Author

*E-mail: Jlou@rice.edu.

Funding

The work at Rice University was supported by the Robert A. Welch Foundation Grant C-1716, the NSF Grant ECCS-1327093, and the U.S. Army Research Office MURI Grant W911NF-11-1-0362.

Notes

The authors declare no competing financial interest.

Biographies

Sina Najmaei is a Ph.D. candidate at Rice University under the supervision of Professor Jun Lou. He earned a M.S. in applied physics from the University of Texas at Austin and a B.S. in physics from Azad University (Tehran, Iran).

Jiangtan Yuan is a Ph.D. student at Rice University under the supervision of Professor Jun Lou. He received his M.S. in Materials Science from the Institute of Metal Research, Chinese Academy of Sciences, and obtained a B.S. in Physics from Shanxi University.

Jing Zhang is currently a Ph.D. student at Rice University under the supervision of Professor Jun Lou. He received his B.E. and M.S. degrees from Tsinghua University.

Pulickel M. Ajayan received his Ph.D. in materials science and engineering from Northwestern University in 1989. Currently he is the Benjamin M. and Mary Greenwood Anderson Professor in Engineer-

DOI: 10.1021/ar500291j
Acc. Chem. Res. 2015, 48, 31−40

ing and the founding Chair of the Department of Materials Science and NanoEngineering at Rice University.

Jun Lou is an Associate Professor in the Department of Materials Science and NanoEngineering at Rice University, with a Ph.D. in Materials Science from Princeton University. He is a recipient of the US Air Force Office of Scientific Research Young Investigator Award and the ORAU Ralph E. Powe Junior Faculty Enhancement Award.

REFERENCES

(1) Mak, K. F.; Lee, C.; Hone, J.; Shan, J.; Heinz, T. F. Atomically Thin MoS2: A New Direct-Gap Semiconductor. *Phys. Rev. Lett.* **2010**, *105*, No. 136805.

(2) Radisavljevic, B.; Radenovic, A.; Brivio, J.; Giacometti, V.; Kis, A. Single-Layer MoS2 Transistors. *Nat. Nano* **2011**, *6*, 147−150.

(3) Lopez-Sanchez, O.; Lembke, D.; Kayci, M.; Radenovic, A.; Kis, A. Ultrasensitive Photodetectors Based on Monolayer MoS2. *Nat. Nano* **2013**, *8*, 497−501.

(4) Mak, K. F.; He, K.; Lee, C.; Lee, G. H.; Hone, J.; Heinz, T. F.; Shan, J. Tightly Bound Trions in Monolayer MoS2. *Nat. Mater.* **2013**, *12*, 207−211.

(5) Cao, T.; Wang, G.; Han, W.; Ye, H.; Zhu, C.; Shi, J.; Niu, Q.; Tan, P.; Wang, E.; Liu, B.; Feng, J. Valley-Selective Circular Dichroism of Monolayer Molybdenum Disulphide. *Nat. Commun.* **2012**, *3*, No. 887.

(6) Mak, K. F.; He, K.; Shan, J.; Heinz, T. F. Control of Valley Polarization in Monolayer MoS2 by Optical Helicity. *Nat. Nano* **2012**, *7*, 494−498.

(7) Zeng, H.; Dai, J.; Yao, W.; Xiao, D.; Cui, X. Valley Polarization in MoS2 Monolayers by Optical Pumping. *Nat. Nano* **2012**, *7*, 490−493.

(8) Splendiani, A.; Sun, L.; Zhang, Y.; Li, T.; Kim, J.; Chim, C.-Y.; Galli, G.; Wang, F. Emerging Photoluminescence in Monolayer MoS2. *Nano Lett.* **2010**, *10*, 1271−1275.

(9) Britnell, L.; Ribeiro, R. M.; Eckmann, A.; Jalil, R.; Belle, B. D.; Mishchenko, A.; Kim, Y.-J.; Gorbachev, R. V.; Georgiou, T.; Morozov, S. V.; Grigorenko, A. N.; Geim, A. K.; Casiraghi, C.; Neto, A. H. C.; Novoselov, K. S. Strong Light-Matter Interactions in Heterostructures of Atomically Thin Films. *Science* **2013**, *340*, 1311−1314.

(10) Sobhani, A.; Lauchner, A.; Najmaei, S.; Ayala-Orozco, C.; Wen, F.; Lou, J.; Halas, N. J. Enhancing the Photocurrent and Photoluminescence of Single Crystal Monolayer MoS2 with Resonant Plasmonic Nanoshells. *Appl. Phys. Lett.* **2014**, *104*, No. 031112.

(11) Kumar, N.; Najmaei, S.; Cui, Q.; Ceballos, F.; Ajayan, P. M.; Lou, J.; Zhao, H. Second Harmonic Microscopy of Monolayer MoS2. *Phys. Rev. B* **2013**, *87*, No. 161403.

(12) Najmaei, S.; Liu, Z.; Zhou, W.; Zou, X.; Shi, G.; Lei, S.; Yakobson, B. I.; Idrobo, J.-C.; Ajayan, P. M.; Lou, J. Vapour Phase Growth and Grain Boundary Structure of Molybdenum Disulphide Atomic Layers. *Nat. Mater.* **2013**, *12*, 754−759.

(13) Zhan, Y.; Liu, Z.; Najmaei, S.; Ajayan, P. M.; Lou, J. Large-Area Vapor-Phase Growth and Characterization of MoS2 Atomic Layers on a SiO2 Substrate. *Small* **2012**, *8*, 966−971.

(14) Liu, K.-K.; Zhang, W.; Lee, Y.-H.; Lin, Y.-C.; Chang, M.-T.; Su, C.-Y.; Chang, C.-S.; Li, H.; Shi, Y.; Zhang, H.; Lai, C.-S.; Li, L.-J. Growth of Large-Area and Highly Crystalline MoS2 Thin Layers on Insulating Substrates. *Nano Lett.* **2012**, *12*, 1538−1544.

(15) Lee, Y.-H.; Zhang, X.-Q.; Zhang, W.; Chang, M.-T.; Lin, C.-T.; Chang, K.-D.; Yu, Y.-C.; Wang, J. T.-W.; Chang, C.-S.; Li, L.-J.; Lin, T.-W. Synthesis of Large-Area MoS2 Atomic Layers with Chemical Vapor Deposition. *Adv. Mater.* **2012**, *24*, 2320−2325.

(16) Perebeinos, V.; Avouris, P. Inelastic Scattering and Current Saturation in Graphene. *Phys. Rev. B* **2010**, *81*, No. 195442.

(17) Ma, N.; Jena, D. Charge Scattering and Mobility in Atomically Thin Semiconductors. *Phys. Rev. X* **2014**, *4*, No. 011043.

(18) Qiu, H.; Xu, T.; Wang, Z.; Ren, W.; Nan, H.; Ni, Z.; Chen, Q.; Yuan, S.; Miao, F.; Song, F.; Long, G.; Shi, Y.; Sun, L.; Wang, J.; Wang, X. Hopping Transport through Defect-Induced Localized States in Molybdenum Disulphide. *Nat. Commun.* **2013**, *4*, No. 2642.

(19) Ghatak, S.; Pal, A. N.; Ghosh, A. Nature of Electronic States in Atomically Thin MoS2 Field-Effect Transistors. *ACS Nano* **2011**, *5*, 7707−7712.

(20) Tsen, A. W.; Brown, L.; Levendorf, M. P.; Ghahari, F.; Huang, P. Y.; Havener, R. W.; Ruiz-Vargas, C. S.; Muller, D. A.; Kim, P.; Park, J. Tailoring Electrical Transport Across Grain Boundaries in Polycrystalline Graphene. *Science* **2012**, *336*, 1143−1146.

(21) Najmaei, S.; Zou, X.; Er, D.; Li, J.; Jin, Z.; Gao, W.; Zhang, Q.; Park, S.; Ge, L.; Lei, S.; Kono, J.; Shenoy, V. B.; Yakobson, B. I.; George, A.; Ajayan, P. M.; Lou, J. Tailoring the Physical Properties of Molybdenum Disulfide Monolayers by Control of Interfacial Chemistry. *Nano Lett.* **2014**, *14*, 1354−1361.

(22) Fivaz, R.; Mooser, E. Electron-Phonon Interaction in Semiconducting Layer Structures. *Phys. Rev.* **1964**, *136*, A833−A836.

(23) Lee, C.; Li, Q.; Kalb, W.; Liu, X.-Z.; Berger, H.; Carpick, R. W.; Hone, J. Frictional Characteristics of Atomically Thin Sheets. *Science* **2010**, *328*, 76−80.

(24) Joensen, P.; Frindt, R. F.; Morrison, S. R. Single-Layer MoS2. *Mater. Res. Bull.* **1986**, *21*, 457−461.

(25) Novoselov, K. S.; Jiang, D.; Schedin, F.; Booth, T. J.; Khotkevich, V. V.; Morozov, S. V.; Geim, A. K. Two-Dimensional Atomic Crystals. *Proc. Natl. Acad. Sci. U. S. A.* **2005**, *102*, 10451−10453.

(26) Tang, D.-M.; Kvashnin, D. G.; Najmaei, S.; Bando, Y.; Kimoto, K.; Koskinen, P.; Ajayan, P. M.; Yakobson, B. I.; Sorokin, P. B.; Lou, J.; Golberg, D. Nanomechanical Cleavage of Molybdenum Disulphide Atomic Layers. *Nat. Commun.* **2014**, *5*, No. 3631.

(27) Ghosh, S.; Najmaei, S.; Kar, S.; Vajtai, R.; Lou, J.; Pradhan, N. R.; Balicas, L.; Ajayan, P. M.; Talapatra, S. Universal ac Conduction in Large Area Atomic Layers of CVD-Grown MoS2. *Phys. Rev. B* **2014**, *89*, No. 125422.

(28) Zhang, J.; Najmaei, S.; Lin, H.; Lou, J. MoS2 Atomic Layers with Artificial Active Edge Sites As Transparent Counter Electrodes for Improved Performance of Dye-Sensitized Solar Cells. *Nanoscale* **2014**, *6*, 5279−5283.

(29) Fivaz, R.; Mooser, E. Mobility of Charge Carriers in Semiconducting Layer Structures. *Phys. Rev.* **1967**, *163*, 743−755.

(30) Zhou, W.; Zou, X.; Najmaei, S.; Liu, Z.; Shi, Y.; Kong, J.; Lou, J.; Ajayan, P. M.; Yakobson, B. I.; Idrobo, J.-C. Intrinsic Structural Defects in Monolayer Molybdenum Disulfide. *Nano Lett.* **2013**, *13*, 2615−2622.

(31) Najmaei, S.; Ajayan, P. M.; Lou, J. Quantitative Analysis of the Temperature Dependency in Raman Active Vibrational Modes of Molybdenum Disulfide Atomic Layers. *Nanoscale* **2013**, *5*, 9758−9763.

(32) Liu, H.; Si, M.; Najmaei, S.; Neal, A. T.; Du, Y.; Ajayan, P. M.; Lou, J.; Ye, P. D. Statistical Study of Deep Submicron Dual-Gated Field-Effect Transistors on Monolayer Chemical Vapor Deposition Molybdenum Disulfide Films. *Nano Lett.* **2013**, *13*, 2640−2646.

(33) Amani, M.; Chin, M. L.; Birdwell, A. G.; O'Regan, T. P.; Najmaei, S.; Liu, Z.; Ajayan, P. M.; Lou, J.; Dubey, M. Electrical Performance of Monolayer MoS2 Field-Effect Transistors Prepared by Chemical Vapor Deposition. *Appl. Phys. Lett.* **2013**, *102*, No. 193107.

(34) Najmaei, S.; Amani, M.; Chin, M. L.; Liu, Z.; Birdwell, A. G.; O'Regan, T. P.; Ajayan, P. M.; Dubey, M.; Lou, J. Electrical Transport Properties of Polycrystalline Monolayer Molybdenum Disulfide. *ACS Nano* **2014**, *8*, 7930−7937.

(35) van der Zande, A. M.; Huang, P. Y.; Chenet, D. A.; Berkelbach, T. C.; You, Y.; Lee, G.-H.; Heinz, T. F.; Reichman, D. R.; Muller, D. A.; Hone, J. C. Grains and Grain Boundaries in Highly Crystalline Monolayer Molybdenum Disulphide. *Nat. Mater.* **2013**, *12*, 554−561.

(36) Radisavljevic, B.; Kis, A. Mobility Engineering and a Metal−Insulator Transition in Monolayer MoS2. *Nat. Mater.* **2013**, *12*, 815−820.

(37) Murphy, D. W.; Hull, G. W. Monodispersed Tantalum Disulfide and Adsorption Complexes with Cations. *J. Chem. Phys.* **1975**, *62*, 973−978.

(38) Bardeen, J. Surface States and Rectification at a Metal Semi-Conductor Contact. *Phys. Rev.* **1947**, *71*, 717−727.

DOI: 10.1021/ar500291j
Acc. Chem. Res. 2015, 48, 31−40

(39) Shockley, W.; Pearson, G. L. Modulation of Conductance of Thin Films of Semi-Conductors by Surface Charges. *Phys. Rev.* **1948**, *74*, 232−233.
(40) Zhu, W.; Low, T.; Lee, Y.-H.; Wang, H.; Farmer, D. B.; Kong, J.; Xia, F.; Avouris, P. Electronic Transport and Device Prospects of Monolayer Molybdenum Disulphide Grown by Chemical Vapour Deposition. *Nat. Commun.* **2014**, *5*, No. 3087.
(41) Yu Z.; Pan, Y.; Shen, Y.; Wang, Z.; Ong, Z.-Y.; Xu, T.; Xin, R.; Pan, L.; Wang, B.; Sun, L.; Wang, J.; Zhang, G.; Zhang, Y. W.; Shi, Y.; Wang, X. Towards Intrinsic Charge Transport in Monolayer Molybdenum Disulfide by Defect and Interface Engineering. 2014 arXiv:cond-mat.mtrl-sci/1408.6614 arXiv.org e-Print archive. http://arxiv.org/abs/1408.6614.
(42) Liu, Z.; Amani, M.; Najmaei, S.; Xu, Q.; Zou, X.; Zhou, W.; Yu, T.; Qiu, C.; Birdwell, A. G.; Crowne, F. J.; Vajtai, R.; Yokobson, B. I.; Xia, Z.; Dubey, M.; Ajayan, P. M.; Lou, J. Strain and structure heterogeneity in MoS2 atomic layers grown by chemical vapour deposition. *Nat. Commun.* **2014**, DOI: 10.1038/ncomms6246.

DOI: 10.1021/ar500291j
Acc. Chem. Res. 2015, 48, 31−40